

# Conductivity anisotropy helps to reveal the microscopic structure of a density wave at imperfect nesting

P. D. Grigoriev

*L. D. Landau Institute for Theoretical Physics, Chernogolovka, 142432, Russia and  
Institut Laue-Langevin, Grenoble, France*

S. S. Kostenko

*Institute of Problems of Chemical Physics, 142432, Chernogolovka, Russia*

Superconductivity or metallic state may coexist with density wave ordering at imperfect nesting of the Fermi surface. In addition to the macroscopic spatial phase separation, there are, at least, two possible microscopic structures of such coexistence: (i) the soliton-wall phase and (ii) the ungapped Fermi-surface pockets. We show that the conductivity anisotropy allows to distinguish between these two microscopic density-wave structures. The results obtained may help to analyze the experimental observations in layered organic metals  $(\text{TMTSF})_2\text{PF}_6$ ,  $(\text{TMTSF})_2\text{ClO}_4$ ,  $\alpha$ -(BEDT-TTF) $_2\text{KHg}(\text{SCN})_4$  and in other compounds.

PACS numbers: 71.30.+h, 74.70.Kn, 75.30.Fv

## I. INTRODUCTION

At imperfect nesting, the charge/spin-density-wave gap in electron spectrum does not cover the whole Fermi surface, so that the density-wave and metallic/superconducting states may coexist. In addition to the macroscopic spatial phase separation,<sup>1</sup> such density-wave state may have two different microscopic structures: (i) spatially uniform structure with reconstructed Fermi surface (FS), containing ungapped parts<sup>2,3</sup> and (ii) spatially non-uniform soliton structure<sup>4-6</sup>. Superconductivity, appearing on such density-wave background is rather common<sup>7,8</sup> and has many unusual properties, including the strong enhancement of the upper critical field<sup>3,6,9,10</sup>, anisotropic transition temperature<sup>11</sup> etc. The knowledge of the microscopic structure of the density wave (DW) state at imperfect nesting is important for describing various compounds, where charge/spin-density wave coexists with metallic/superconducting states. For all above scenarios the metallic conductivity decreases but does not vanish after the transition to density-wave state. This decrease of conductivity may be anisotropic<sup>12</sup> and depend on the DW microscopic structure. In the present report we show how this anisotropy can help to distinguish various DW microscopic structures. These results may be useful to describe the electronic properties of organic metals  $\alpha$ -(ET) $_2\text{MHg}(\text{SCN})_4$  with  $M = \text{K}$  and  $\text{Tl}$ ,  $(\text{TMTSF})_2X$  with  $X = \text{PF}_6$  or  $\text{ClO}_4$ , and of other compounds.

For  $(\text{TMTSF})_2\text{PF}_6$  there are several arguments in favor of a macroscopic phase separation<sup>1</sup> rather than soliton<sup>4,5,13-16</sup> scenario. The main of these arguments is the constant (pressure independent) transition temperature  $T_c^{\text{SC}}$  to the superconducting (SC) state, which is almost the same in the uniform (high-pressure) and nonuniform (coexistent) superconducting state. This is not the case for  $\alpha$ -(ET) $_2\text{MHg}(\text{SCN})_4$  organic metals, where the soliton-wall scenario is more probable. The other arguments in favour of macroscopic phase separation in  $(\text{TMTSF})_2\text{PF}_6$  in Ref.<sup>1</sup> involve magnetic field, which changes the soliton phase in the presence of imperfect nesting and may even lead to a field-induced spin-

density wave (FISDW) with soliton microscopic structure. Although some theoretical results on the evolution of the soliton DW structure in magnetic field have been obtained for ideally 1D conductor<sup>17</sup>, there is no theoretical study of the soliton DW microscopic structure in magnetic field in the presence of imperfect nesting. The NMR absorption lineshape<sup>18</sup> also suggests the soliton DW structure rather than macroscopic domains with usual uniform DW. Moreover, SC appearing in the soliton wall phase of spin-density wave (SDW) has the triplet SC pairing<sup>16</sup> in agreement with experiments in  $(\text{TMTSF})_2\text{PF}_6$ .<sup>19</sup> From energy considerations, the soliton wall scenario<sup>4,5,13-16</sup> is more favorable, because the energy loss  $W$  due to nonuniform DW order parameter is compensated by the large kinetic energy of soliton-band quasiparticles<sup>13,15</sup>. Thus, the question about the DW structure in  $(\text{TMTSF})_2\text{PF}_6$  in the coexistence region is still open. The "double" spatial separation is also possible, where there are macroscopic domains of metallic and soliton DW states.

## II. TEMPERATURE DEPENDENCE OF CONDUCTIVITY ANISOTROPY IN QUASI-1D CONDUCTORS WITH IMPERFECT NESTING

The quasi-1D free electron dispersion without magnetic field has the form

$$\varepsilon(\mathbf{k}) = \pm v_F(k_x \mp k_F) + t_{\perp}(\mathbf{k}_{\perp}), \quad (1)$$

where the interchain dispersion  $t_{\perp}(\mathbf{k}_{\perp})$  is much weaker than the in-plane Fermi energy  $E_F \sim v_F k_F$  and given by the tight-binding model with few leading terms:

$$t_{\perp}(\mathbf{k}_{\perp}) = 2t_b \cos(k_y b) + 2t'_b \cos(2k_y b). \quad (2)$$

Here  $b$  is the lattice constants in the  $y$ -direction, and usually  $t'_b \ll t_b \ll t_a \sim v_F k_F$ . The dispersion along the  $z$ -axis is considerably weaker than along the  $y$ -direction and is omitted. The FS consists of two warped sheets and possesses an approximate nesting property,  $2\varepsilon_{+}(\mathbf{k}) \equiv$

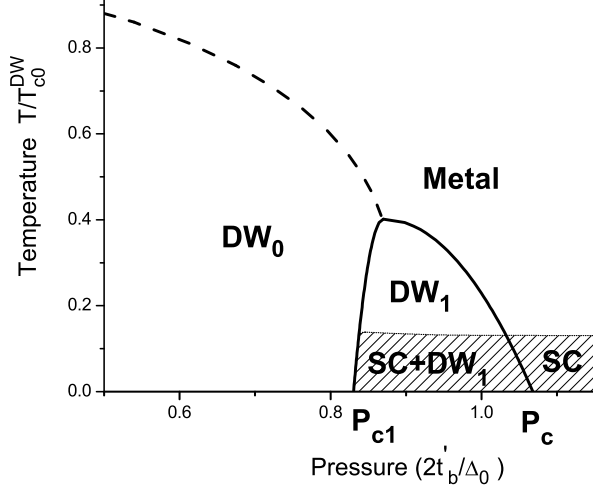


FIG. 1: The schematic picture of the phase diagram in organic metals, where metal/superconducting state coexists with DW in some pressure interval above  $P_{c1}$  but below  $P_c$ .  $DW_0$  stands for the uniform fully gapped DW.  $DW_1$  denotes the DW state when the imperfect nesting term  $2t'_b > \Delta_0$ , so that the ungapped FS pockets or nonuniform DW structure appear.

$\varepsilon(\mathbf{k}) + \varepsilon(\mathbf{k} - \mathbf{Q}_N) \sim t'_b \ll E_F$ , with  $\mathbf{Q}_N \approx (2k_F, \pi/b)$  being the nesting vector. The nesting property leads to the formation of DW at low temperature and is only spoiled by the second term  $t'_b(k_y)$  in Eq. (2), which, therefore, is called the "anti-nesting" term. Increase of the latter with applied pressure leads to the transition in the  $DW_1$  state at  $P > P_{c1}$  (see Fig. 1 below or Fig. 1 in Refs.<sup>3,6</sup>), where the quasi-particle states on the Fermi level first appear and lead to the metallic conductivity or to SC instability at low temperature  $T < T_c^{SC}$ . In the pressure interval  $P_{c1} < P < P_c$  the new state develops, where the DW coexists with superconductivity at rather low temperature  $T < T_c^{SC}$ , while at higher temperature  $T_c^{SC} < T < T_c^{DW}$  the DW state coexists with the metallic phase. This coexistence takes place via macroscopic phase separation<sup>1</sup>, via the formation of small ungapped pockets<sup>3</sup> or via the soliton phase<sup>14,15</sup>. In most DW superconductors, the DW transition temperature is much greater than the SC transition temperature,  $T_c^{DW} \gg T_c^{SC}$ . For example, in  $(\text{TMTSF})_2\text{PF}_6$   $T_c^{SDW} \approx 8.5\text{K} \gg T_c^{SC} \approx 1.1\text{K}$ , and in  $\alpha\text{-(BEDT-TTF)}_2\text{KHg(SCN)}_4$ ,  $T_c^{CDW} \approx 8\text{K} \gg T_c^{SC} \approx 0.1\text{K}$ . Below we consider the temperature interval  $T_c^{SC} < T < T_c^{DW}$ , i.e. the state with metallic conductivity.

In the  $\tau$ -approximation, the conductivity along the main axes is given by<sup>22</sup>:

$$\sigma_i(T) = e^2 \tau \sum_{\mathbf{k}} v_i^2(\mathbf{k}) (-n'_F[\varepsilon(\mathbf{k})]), \quad (3)$$

where  $e$  is the electron charge,  $\tau$  is the mean free time,  $\mathbf{k}$  is electron momentum,  $v_i$  is the component of the electron velocity along the  $i$ -direction,  $n'_F(\varepsilon) = -1/\{4T \cosh^2[(\varepsilon - \mu)/2T]\}$  is the derivative of the Fermi distribution function, which restricts the summation over

momentum to the vicinity of FS,  $\mu$  is the chemical potential, and  $\varepsilon(\mathbf{k})$  is the electron dispersion. The electron velocity is calculated from Eq. (1) using

$$v_i(\mathbf{k}) = \partial \varepsilon(\mathbf{k}) / \partial k_i. \quad (4)$$

Since the electron dispersion differs for various DW structures, so does the temperature dependence of conductivity anisotropy  $\sigma_i/\sigma_j$ . Now we consider this anisotropy for the initial electron dispersion given by Eqs. (1) and (2).

### A. DW state with open FS pockets

The electron dispersion in the DW state with imperfect nesting and open FS pockets for the initial electron dispersion given by Eqs. (1) and (2) was studied in Ref.<sup>3</sup>. There are eight elongated open FS pockets in this case, four pockets per each FS sheet (see Fig. 2 or Fig. 2 in Ref.<sup>3</sup>). The in-plane conductivity anisotropy is determined by the two inclined FS pockets, marked by numbers 3 and 4, in this figure. The tangent of the inclination angle  $\phi$  of these pockets (see Fig. 2) approximately gives the ratio  $\langle v_y^2 \rangle / \langle v_x^2 \rangle \sim \tan^2 \phi \approx (t_b/t_a)^2$ , where the angular brackets mean averaging over FS. Thus, in the DW state one expects the anisotropy ratio

$$\sigma_y/\sigma_x \approx \langle v_y^2 \rangle / \langle v_x^2 \rangle \sim \tan^2 \phi \sim (t_b/t_a)^2 \ll 1, \quad (5)$$

which is close to the anisotropy without DW and slightly depends on pressure. The change of this anisotropy ratio due to the transition to DW is small for this scenario of the microscopic DW structure.

### B. Soliton-wall density-wave state

In the soliton phase the DW order parameter depends on the coordinate along the conducting chains:  $\Delta(x) \approx \Delta_0 \text{sn}(x/\xi_{DW})$ , where  $\text{sn}(y)$  is the elliptic sinus function. As a result an array of soliton walls of width  $\xi_{DW} = \hbar v_F / \pi \Delta_0$  gets formed, where the DW order parameter changes sign. Each soliton wall contributes one electron-like quasiparticle per conducting chain on the Fermi level. For rather high soliton-wall linear concentration  $n_s$  the quasiparticles on different soliton walls couple and form new conducting band in the middle of the DW energy gap. The dispersion in this soliton band is<sup>13,15</sup>

$$E(\mathbf{k}) = E(k_x) + \varepsilon_+(k_y), \quad (6)$$

where the interchain part of the dispersion is given by the anti-nesting term in the dispersion (2):

$$\varepsilon_+(\mathbf{k}_\perp) = [t_\perp(\mathbf{k}_\perp) + t_\perp(\mathbf{k}_\perp - \mathbf{Q}_\perp)] / 2 \approx 2t'_b \cos(2k_y b). \quad (7)$$

The dispersion  $E(k_x)$  along the conducting chains was found in Ref.<sup>21</sup> (see Fig. 1 in Ref.<sup>21</sup>), and for qualitative analysis it can be approximated by

$$E(k_x) \approx E_- \sin[\pi(|k_x| - k_F)/2\kappa_0]. \quad (8)$$

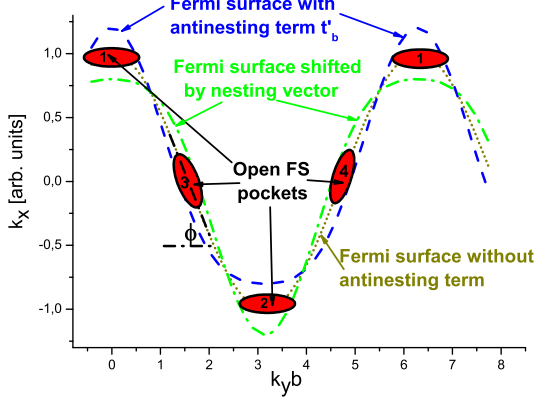


FIG. 2: (Color online) The schematic picture of small open pockets on one Fermi surface sheet, which get formed when the anti-nesting term  $2t'_b$  in Eq. (2) exceeds the DW energy gap  $\Delta_0$ . The blue dashed line shows the Fermi surface sheet with imperfect nesting, i.e. with  $2t'_b > \Delta_0$ . The green dash-dotted line shows the other Fermi surface sheet shifted by the nesting vector. If the nesting was perfect, these two lines would coincide. The dotted brown line shows the perfectly nested Fermi surface sheet. The red solid ellipses are the small Fermi surface pockets, that appear in the DW state when  $2t'_b > \Delta_0$ , i.e. when pressure exceeds  $P_{c1}$ .

The soliton band width  $E_-$  and boundary  $\kappa_0 = \pi n_s/2$  in the momentum space are related to the linear concentration  $n_s$  of the soliton walls<sup>21</sup>, which strongly depends on the anti-nesting electron dispersion and, hence, on applied pressure. At small soliton concentration  $n_s \rightarrow 0$  (see Ref.<sup>4</sup>, p. 165):

$$E_- \approx 4\Delta_0 \exp(-\Delta_0/\hbar v_F n_s), \quad (9)$$

while at large soliton concentration  $n_s \sim 1/\xi_{DW}$   $E_- \sim \Delta_0$ . To find  $E_-$  and its pressure dependence one need to minimize the total energy of soliton phase (see Appendix).

Substituting Eqs. (6)-(8) to Eqs. (4) and (5) we obtain the mean square velocity in the soliton phase

$$\langle v_y^2 \rangle \approx 2(t'_b/\hbar)^2, \quad \langle v_x^2 \rangle \approx (\pi E_-/2\hbar\kappa_0)^2/2, \quad (10)$$

and the conductivity anisotropy

$$\sigma_y/\sigma_x \approx \langle v_y^2 \rangle / \langle v_x^2 \rangle \sim 16(t'_b b \kappa_0 / \pi E_-)^2. \quad (11)$$

At  $t'_b \ll \Delta_0$  all electron states on the Fermi level are gapped by a uniform DW, while at  $t'_b \gg \Delta_0$  the normal-metal or electron-pocket DW state are, usually, more favorable than the soliton DW state. Hence, typically, in the soliton-wall non-uniform DW state  $t'_b \sim \Delta_0$ . Then the ratio  $\sigma_y/\sigma_x \sim 16(t'_b b \kappa_0 / \pi E_-)^2 \gtrsim 1$  even at large soliton concentration  $n_s$ , when  $E_- \sim \Delta_0 \sim 2t'_b$ . Hence, contrary to the FS-pocket scenario, the formation of DW with soliton structure leads to the strong change and even to the inversion of the in-plane conductivity anisotropy. This allows to distinguish experimentally these two microscopic structures of the DW with imperfect nesting.

### C. Macroscopic phase separation

For metal-DW phase separation in the form of macroscopic domains,<sup>1</sup> the calculation of conductivity anisotropy depends strongly on the shape, size and mutual orientation of these domains. If the metallic domains are weakly connected, one encounters the percolation regime. Therefore, it is impossible to propose a general formulas for conductivity anisotropy in this regime without specification of the particular domain geometry. However, the change of the domain shape from filaments to the walls, proposed in Refs.<sup>1,11</sup> to explain the  $T_c^{SC}$  anisotropy, also affects the metallic conductivity anisotropy, which can be easily measured. This issue requires additional experimental and theoretical investigation.

### III. CONCLUSIONS

We have shown that the change of conductivity anisotropy during the transition to the DW state can reveal the microscopic structure of this DW state. This is important in the case of imperfect nesting, when the DW state has metallic conductivity due to the ungapped electronic states on the Fermi level. In particular, for the soliton DW structure<sup>4,5,13-16</sup> the DW transition leads to the strong change and sometimes to the inversion of the in-plane conductivity anisotropy [see Eq. (11)]. On contrary, for the FS-pocket scenario<sup>3</sup> of metal-DW coexistence the in-plane anisotropy only slightly changes. This allows to experimentally distinguish these two microscopic DW structures, which may be useful to describe the electronic properties of organic metals, such as  $\alpha$ -(ET)<sub>2</sub>MHg(SCN)<sub>4</sub> with M = K or Tl and (TMTSF)<sub>2</sub>X with X = PF<sub>6</sub> or ClO<sub>4</sub>, and of various high-temperature superconductors, where charge/spin-density wave coexists with superconducting/metallic state. For macroscopic phase separation the conductivity anisotropy strongly depends on the geometry and concentration of the metallic domains, which requires investigation of the particular compounds.

The work was supported by SIMTECH Program (Grant No. 246937), by RFBR Grant No. 13-02-00178, by the Theoretical Center for the Physics in Grenoble, and by the program "Strongly correlated electron-phonon systems" of the Physics Branch of RAS.

#### Appendix A: Energy of soliton phase and the pressure dependence of the electron-band width in this phase

The energy of the soliton phase is (see Eqs. (33)-(35) of Ref.<sup>13</sup> or Eqs. (9)-(12) of Ref.<sup>15</sup>)

$$W_{SP} = -\frac{\Delta_0^2}{2\pi\hbar v_F} + n_s A(t'_b) + n_s E_-^2 B, \quad (A1)$$

where the energy cost of a soliton wall per chain is (we denote  $\varepsilon_{\pm}(\mathbf{k}_{\perp}) = [t_{\perp}(\mathbf{k}_{\perp}) \pm t_{\perp}(\mathbf{k}_{\perp} - \mathbf{Q}_{\perp})]/2$ ):

$$A(t'_b) = (2/\pi)\Delta_0 - 2 \int_{t_{\perp} \leq 0} \varepsilon_+(k_y) b dk_y / 2\pi, \quad (\text{A2})$$

and the interaction between the soliton walls is given by

$$B(t'_b) \approx \frac{1}{2\pi\Delta_0} - \sum_{FS} \frac{b/2\pi}{|d\varepsilon_+/dk_y|_0}, \quad (\text{A3})$$

where  $|d\varepsilon_+/dk_y|_0$  is the value of the transverse velocity at the four values of  $p_{\perp}$  where  $t'_b(k_y) = 0$ . At  $B > 0$ , crossing the point  $A(t'_b) = 0$  corresponds to the second-order transition from the "homogeneous" SDW to the soliton walls lattice with the soliton wall concentration  $n_s$  gradually increasing from zero. Negative  $B < 0$  would mean an abrupt first-order phase transition at  $P = P_{c1}$ , when the soliton concentration  $n_s$  jumps to some finite value.<sup>13</sup> The soliton band boundary in the momentum space has linear smallness,  $\kappa_0 = \pi n_s/2$ , and the soliton band width is exponentially small for small  $n_s$ . Differentiating of Eq. (A1) with respect to  $E_-$  gives the optimal value of  $E_-$  that minimizes the energy (A1):

$$E_-^2 = -A(t'_b) / \left[ B(t'_b) (2 \ln(4\Delta_0/E_-) + 1) \right]. \quad (\text{A4})$$

This width depends strongly on the dispersion  $\varepsilon_+(k_y)$  in the soliton band. For the dispersion (2) Eqs. (A2),(A3)

give

$$A(t'_b) = (2/\pi)(\Delta_0 - 2t'_b), \quad (\text{A5})$$

$$B(t'_b) = \frac{1}{2\pi\Delta_0} - \frac{1}{4\pi t'_b}. \quad (\text{A6})$$

The occasional degeneracy, meaning that both  $A(t'_b)$  and  $B(t'_b)$  become zero at the same point  $2t'_b = \Delta_0$ , is a consequence of the particular electron dispersion (2). In real compounds this degeneracy is always removed by higher harmonics in the dispersion (2). In the presence of the occasional degeneracy (A6), the width of the soliton band at  $P \rightarrow P_{c1}$  (i.e., at  $\Delta_0 \rightarrow 2t'_b$ ) reduces very slowly:

$$E_- \approx \frac{2\Delta_0}{\sqrt{2 \ln(4\Delta_0/E_-) + 1}} \sim \Delta_0, \quad (\text{A7})$$

which means a sharp (though second-order) transition from the uniform DW to the soliton phase. Without the occasional degeneracy (A5),(A6)

$$E_- \sim \sqrt{\Delta_0 \delta} \equiv \sqrt{\Delta_0 (2t'_b - \Delta_0)} \propto \sqrt{P - P_{c1}}. \quad (\text{A8})$$

A quantitative estimate of the dependence  $E_-(P)$  requires a more accurate calculation of the interaction (A3) between soliton walls.

- 
- <sup>1</sup> Arjun Narayanan, Andhika Kiswandhi, David Graf, James Brooks, and Paul Chaikin, Phys. Rev. Lett. **112**, 146402 (2014).
- <sup>2</sup> P. Monceau, Adv. Phys. **61**, 325 (2012).
- <sup>3</sup> P.D. Grigoriev, Phys. Rev. B **77**, 224508 (2008).
- <sup>4</sup> S.A. Brazovskii and N.N. Kirova, Sov. Sci. Rev. A Phys., **5**, 99 (1984).
- <sup>5</sup> W.P. Su and J. R. Schrieffer, *Physics in One Dimension*/ Ed. by J. Bernasconi and T. Schneider, Springer series in Solid State Sciences, Berlin, Heidelberg and New York: Springer, 1981.
- <sup>6</sup> P.D. Grigoriev, Physica B **404**, 513 (2009).
- <sup>7</sup> A.M. Gabovich, A.I. Voitenko, J.F. Annett and M. Ausloos, Supercond. Sci. Technol. **14**, R1-R27 (2001); A.M. Gabovich, A.I. Voitenko and M. Ausloos, Physics Reports **367**, 583–709 (2002).
- <sup>8</sup> T. Vuletic, P. Auban-Senzier, C. Pasquier et al., Eur. Phys. J. B **25**, 319 (2002).
- <sup>9</sup> I. J. Lee, P. M. Chaikin, and M. J. Naughton, Phys. Rev. Lett. **88**, 207002 (2002).
- <sup>10</sup> D. Andres, M. V. Kartsovnik, W. Biberacher, K. Neumaier, E. Schuberth, and H. Müller, Phys. Rev. B **72**, 174513 (2005).
- <sup>11</sup> N. Kang, B. Salameh, P. Auban-Senzier, D. Jerome, C.R. Pasquier, and S. Brazovskii, Phys. Rev. B **81**, 100509(R) (2010).
- <sup>12</sup> A.A. Sinchenko, P.D. Grigoriev, P. Lejay, P. Monceau, Phys. Rev. Lett. **112**, 036601 (2014).
- <sup>13</sup> S.A. Brazovskii, L.P. Gor'kov, A.G. Lebed', Sov. Phys. JETP **56**, 683 (1982) [Zh. Eksp. Teor. Fiz. **83**, 1198 (1982)].
- <sup>14</sup> L.P. Gor'kov, A. G. Lebed, J. Phys. Colloq. Suppl. **44**, C3-1531 (1983).
- <sup>15</sup> L.P. Gor'kov, P.D. Grigoriev, Europhys. Lett. **71**, 425 (2005).
- <sup>16</sup> L.P. Gor'kov, P.D. Grigoriev, Phys. Rev. B **75**, 020507(R) (2007).
- <sup>17</sup> S. A. Brazovskii, I. E. Dzyaloshinskii, and N. N. Kirova, JETP **54**, 1209 (1981).
- <sup>18</sup> I. J. Lee, S. E. Brown, W. Yu, M. J. Naughton, and P. M. Chaikin, Phys. Rev. Lett. **94**, 197001 (2005).
- <sup>19</sup> I. J. Lee, M. J. Naughton, G. M. Danner, and P. M. Chaikin, Phys. Rev. Lett. **78**, 3555 (1997); I. J. Lee, P. M. Chaikin, and M. J. Naughton, Phys. Rev. B **62**, R14 669 (2000); I. J. Lee, S. E. Brown, W. G. Clark, M. J. Strouse, M. J. Naughton, W. Kang, and P. M. Chaikin, Phys. Rev. Lett. **88**, 017004 (2001); I.J. Lee, D. S. Chow, W. G. Clark, M. J. Strouse, M. J. Naughton, P. M. Chaikin, and S. E. Brown, Phys. Rev. B **68**, 092510 (2003).
- <sup>20</sup> L. P. Gor'kov and A.G. Lebed', J. Phys. (Paris) **44**, C3-1531 (1983).
- <sup>21</sup> S.A. Brazovskii, S.A. Gordyunin and N.N. Kirova, JETP Lett. **31**, 451 (1980)[Pis'ma v ZhETF **31**, 486 (1980)].
- <sup>22</sup> A.A. Abrikosov, *Fundamentals of the theory of metals*, North-Holland, 1988.